INFLUENCE RANGE SIMULATION OF LOOSE BLASTING BOREHOLE IN THE COAL-ROCK MASS

by

Hong LI [a,b], ***Ming-Ju LIU*** [a], ***Hong-Wei YANG*** [c,d], ***Hong GAO*** [c,d], ***and Tong-Qiang XIA*** [b,e*]

[a] School of Safety Science and Engineering, Henan Polytechnic University, Jiaozuo, China
[b] Hebei State Key Laboratory of Mine Disaster Prevention, North China Institute of Science and Technology, Beijing, China
[c] Shengyang Research Institute, China Coal Technology and Engineering Group, Shengyang, China
[d] State Key Laboratory of Coal Mine Safety Technology, Fushun, China
[e] Chinese Academy of Science, Institute Rock and Soil Mechanics, State Key Laboratory of Geomechanic and Geotechnical Engineering, Wuhan, China

Original scientific paper
https://doi.org/10.2298/TSCI180607211L

The influence scope of the blasting borehole is the key factor to the construction of loose blasting measures. A non-linear numerical model considering the multi-physical coupling factors, including in-situ stress, coal damage, and gas migration, etc., is established, and the model is solved by Comsol Multiphyscics software. The influence range of gas migration is analyzed, and the influence scope is determined to be between 3.5 m and 4.0 m. The change law of gas concentration and gas volume in test boreholes around blasting boreholes are investigated, and the effective influence range of loose blasting is about between 3.5 m and 4.0 m. The consistency between field test and numerical simulation results show that the effective influence range of loose blasting can be regard as about 3.5 m. The conclusions of this study provide an effective solution for improving the effect of loose blasting as a local anti-penetration measure and determining the reasonable parameter of hole placement.

Key words: *loose blasting, effective influence range, multi-physical coupling, gas migration, elasticity modulus*

Introduction

With the increasing number of high gas and prominent mines in China, the difficulty of mine gas control was further increasing [1, 2]. For high-gas, low-permeability and coal-gas accidents always took place, which are caused by inadequate anti-penetration measures [3]. Loose blasting, namely, as a local comprehensive measure to prevent coal and gas outburst, had a good effect in enhancing the permeability of coal seams [4-7]. It had been used in Beipiao and Lianshao mining areas as early as the mid 1960 in mining areas. In recent years, it had been widely used in the field of local measures to prevent coal and gas outburst of excavation faces [8, 9]. The initiation and propagation processes of cracks through different mechanisms were studied by using simulation [10]. The fractal deep-hole blasting and its induced stress behavior of hard roof strata in Bayangaole coal mine of China was studied by LS-DYNA simulation software [11]. Using the methods of simulation and on-site observation, the effect of loose blasting

* Corresponding author, e-mail: xt_032485@126.com

on the pressure relief was investigated [12]. Recently, some scholars analysed the effective influence range of loose blasting and the spacing parameter of blasting borehole is proposed [13, 14]. However, the influence of multi-physics coupling factors on blasting boreholes remains to be reported. The factors include elastic mechanics, coal-rock damage and gas migration. However, many researches were usually lack of field engineering verification. Therefore, using numerical simulation and engineering verification methods to study on the effective influence range of loose blasting, so as to provide theoretical reference for more efficient use of loose blasting measures to improve the permeability of coal seam and prevent coal and gas outburst accidents.

Mathematical model

Elastic mechanics equation

Since the loose blasting is a transient process, the time term is not taken into account in the balance equation of effective stress. The deformation equation can be described:

$$\sigma'_{ij,j} + (\alpha\rho\delta_{ij}),\ \ j + f_i = 0 \tag{1}$$

where $\sigma_{ij,j}$ is the stress tensor and f_i – the volume force.

Gas seepage equation

The gas seepage equation including the gas ad/desorption process, can be described [2]:

$$\beta\left[\frac{\phi}{p_0} - \frac{a_1 a_1^2 \rho_s}{2\left(1+a_2 p\right)} + \frac{a_1 a_2 \rho_s}{1+a_2 p}\right]\frac{\partial p^2}{\partial p} - \nabla\left(\beta\frac{k_g}{u_g}\nabla p^2\right) = Q_p \tag{2}$$

Dynamic damage to the stiffness

The damage parameter, D, can be represented as a function of acoustic attenuation coefficient and strain rate. The law of damage development can be revealed through the evolution of α and ξ, and the dynamic damage of rock is judged jointly by the volume stress criterion and the maximum principal stress criterion [15]:

$$\begin{cases} D = \dfrac{8\alpha}{9h}\left(\dfrac{1-\overline{v}^2}{1-2v}\right)\left(\dfrac{\sqrt{20}k_{IC}}{\rho C\xi}\right) & (\sigma_H > 0) \\ D = 1 & (\sigma_H > 0,\ \sigma_{\max} \geq \sigma_t) \end{cases} \tag{3}$$

where h is a constant, $\overline{v} = \exp[-(16/9)\,\beta C_d]$, v – the Poisson's ratio, β – the constant, controlling material unloading and reloading behavior, c_d – the crack density, k_{IC} and C – the material's toughness and the longitudinal wave velocity, respectively, ρ – the density, σ_H – the volume stress, and σ_t – the tensile strength.

Coal rock mass deformation model

The equation of coal and rock mass motion is expressed:

$$(\lambda + \mu)S_{j,ij} + \mu S_{j,ij} + F_j = 0\ \ (i, j = 1, 2) \tag{4}$$

where $\lambda + \mu$ is the elastic constant of Lame, F – the external load, and S – the displacement of the joint of coal and rock mass.

Equations (1)-(4) constitute a multi-physical coupling model of loose blasting.

Numerical simulation

Physical model and boundary conditions

The schematic diagrams of borehole lay-out and the simplified 3-D numerical model are shown in fig. 1. The integral model is set as 10 m × 5 m × 7 m in the *x*-, *y*-, *z*-directions. The basic simulation parameters of gas drainage and loose blasting are listed in tab. 1.

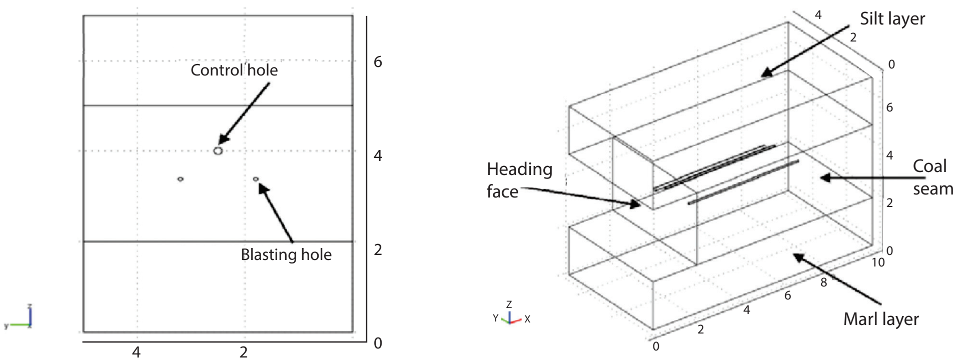

Figure 1. Schematic diagram of borehole layout and physical model of loose blasting

Table1. Basic parameters of gas drainage and loose blasting simulation

Parameter	Value	Parameter	Numerical value
Standard atmospheric pressure	0.1013 MPa	Rock bulk density	2.5×10^3 kgm^{-3}
Gas drainage negative pressure	5000 Pa	Poisson's ratio of coal	0.3
Coal density	1250 kgm^{-3}	Elastic Modulus	1000 MPa
Adsorption gas volume	0.03817 m^{3}kg^{-1}	Porosity free from external forces	5.0%
Adsorption constant	7900 Pa^{-1}	Residual porosity under high compression state	2.0%
Permeability stress sensitivity coefficient	5.0×10^{-8} Pa^{-1}	Pressure coefficient of pore water	1.0
Gas dynamic viscosity	1.84×10^{-5} Pa·s	Compression factor [kgm^{-3}Pa^{-1}]	1.18×10^{-5} kgm^{-3}Pa^{-1}
Original gas pressure	0.98 MPa	Elastic Modulus	10000 MPa
Coal compressive strength	10 MPa	Rock poisson	0.27
Coal compression ratio	15	Friction angle	38 °C
Uniaxial compressive strength	200 MPa	Pull-to-pressure ratio	8
Rock friction angle	30 °C	Explosive gas static pressure	2275.91 MPa

Simulation results

In fig. 2, the broken area is described by blue and the loose area is described by green. Blasting is actually a complicated process of combustion and detonation. Since the expansion of gas with high pressure and high temperature generated by explosion, the damage of the surrounding medium can take place. Due to the difficulty in simulating the actual blasting process, the equivalent bursting pressure of 2275.91 MPa is applied for simulation in radial direction. The loose blasting causes a loose zone with an influence range of about 1.2 m and a crushing zone with a range of 1.05 m around the blasting hole. These results show that loose blasting plays a role in preventing coal and gas outburst accidents.

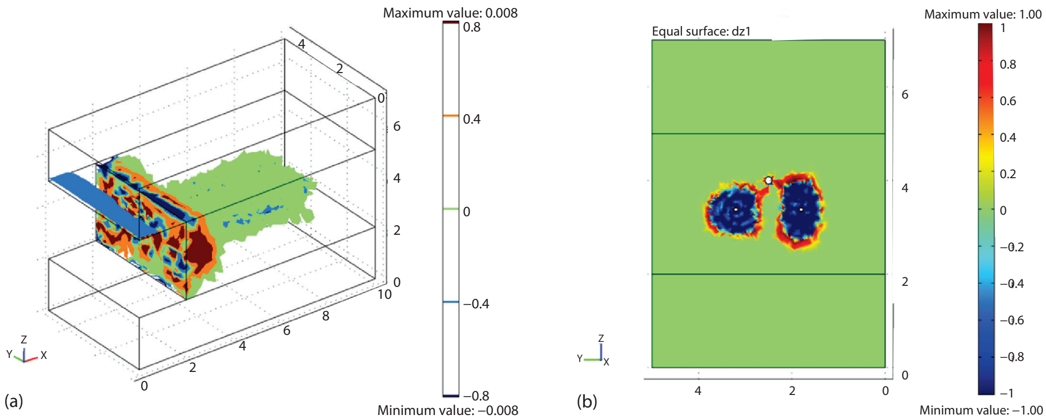

Figure 2. Damage distribution after loose blasting; (a) damage area, (b) damage distribution around borehole

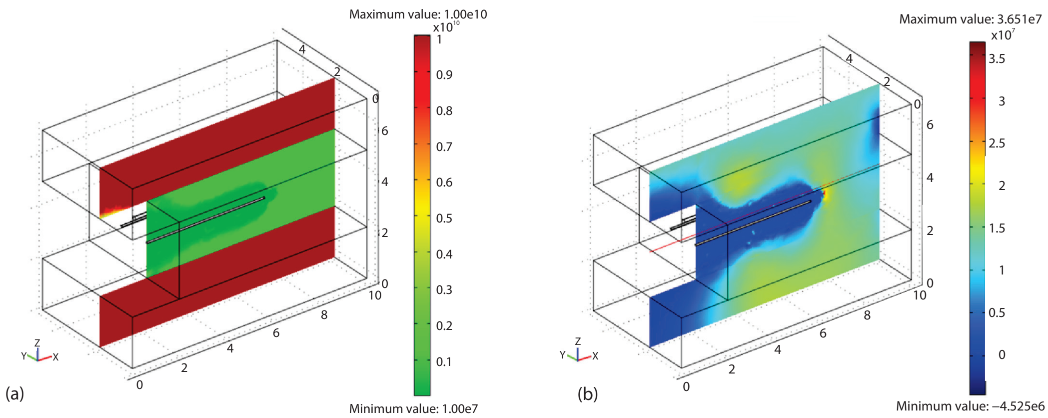

Figure 3. Elastic modulus and stress distribution along the longitudinal profile of the blasting hole; (a) elastic modulus, (b) stress cloud map

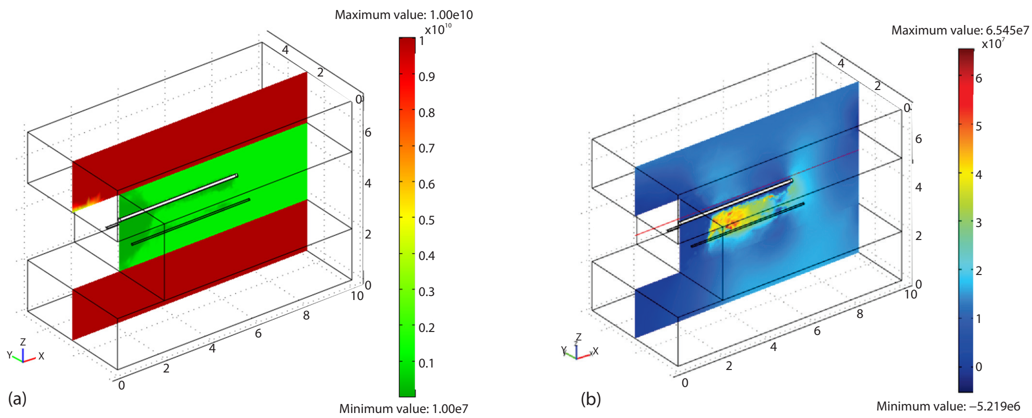

Figure 4. Elastic modulus and stress profile along the control borehole; (a) elastic modulus (b) stress cloud map

Figures 3 and 4 are the elastic modulus and stress distribution diagrams, which are along the longitudinal section of the blasting and control holes, respectively. As shown in fig. 3(b), the blue region in z-axis direction of normal stress is zero which is significantly larger than the range before the loose blasting. The maximum compressive stress is 36.51 MPa, and the maximum tensile stress is 4.525 MPa. The concentration stress of the coal wall is near the blasting hole. It can be seen from fig. 4(a) that the elastic modulus value of green area is 1000 MPa. In the region near the blasting hole, the elastic modulus reduces significantly.

Figure 5(a) shows the stress distribution in tensile lines above the blasting hole. The x-axis value in the 0-2.0 m width range belongs to the working face, and 2.0-10.0 m belongs to the coal seam. Due to the mining damage, the concentration stress in the coal seam is transferred to the inner part of the coal seam, therefore, the stress increases slowly in x-axial direction between 2.0 m and 2.5 m. Between 2.5 m and 9.0 m segment of x-axial, the stress in the z-direction increases significantly, stress reaches its peak when the x-axis value is 3.06 MPa. That is, under the mining conditions, the stress is the highest at 1.06 m from the working surface, and the value is 38.95 MPa. Exceeding working face 9 m is regarded as the normal stress zone, and the stress of 11.86 MPa.

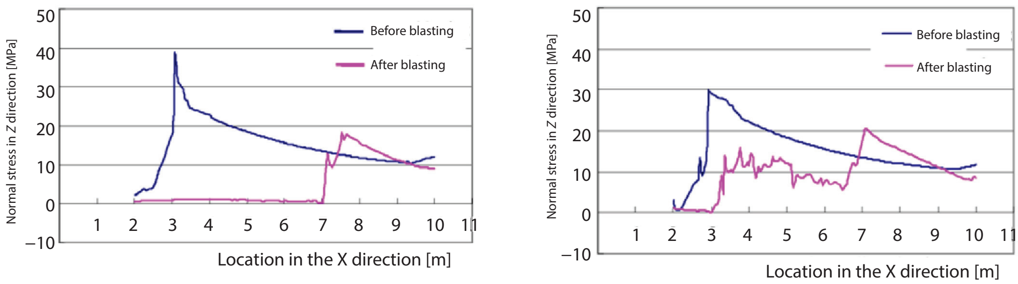

Figure 5. Stress variation curves in tensile lines above the blasting and control holes; (a) the blasting hole, (b) the control hole

Figure 5(b) shows the stress distribution in tensile lines above the control hole. After the loose blasting, the range of the stree relief zone is between 2.0 m and 7.08 m in x-axial direction, where the stress change is about 1.0 MPa, and the concentration stress zone is between 7.33 m and 9.39 m in x-axial direction. When x-axis value is 7.53 m, namely exceeding working face 5.06 m, the positive stress in the z-direction reaches the peak value of 18.3 MPa. In the region of 3.31 m and 9.6 m in x-axial direction, there is a significant increase in z-stress gradient change of stress concentration zone, and the stress reaches its peak when the x-axis value is 7.08 m in the z-axis direction. That is to say, the stress peak is generated at the position of 5.08 m exceeding the working surface, and the value is 20.6 MPa.

From the comparison of the z-direction normal stress curve before and after blasting, it can be seen that the stress relief zone, the concentrated stress zone and primary stress zones can be produced in the front of the working face during mining. After loose blasting, the concentrated stress zone of the coal body moves backward, width of relief zone was increased, peak of normal stress in the z-axis direction was decreased, playing the role of preventing gas outburst accidents. It can be seen that the change of the stress peak makes the stress transfer to the deep zone between 3.5 m and 4.0 m before and after blasting, which enhances the ability of resisting the coal and gas outburst. It can be considered that the impact range of the blasting hole reaches between 3.5-4.0 m.

In-situ measurement

The blasting hole is Ø42 m in diameter and 5.0 m in depth. The charge of each hole is between 4.0 and 6.0 coils/hole, the drilling direction of loose blasting is parallel to the coal seam and the QSJ-90A anti-drilling rig is used for drilling. The third-stage emulsion explosives allowed in the coal mine are selected. The length of each explosive is 0.5 m, the diameter of the grain is 0.06 m, each roll of explosives' weighs is 1.7 kg. The medicine roll is send to the charging position by the wooden cannon-stick with fired medicine (Ø0.055 m $\times$ 1.5 m). The MFB-100B type blasting device is used to detonate one charge and one detonated. The lay-out parameters of specific blasting and test holes are shown in the fig. 6.

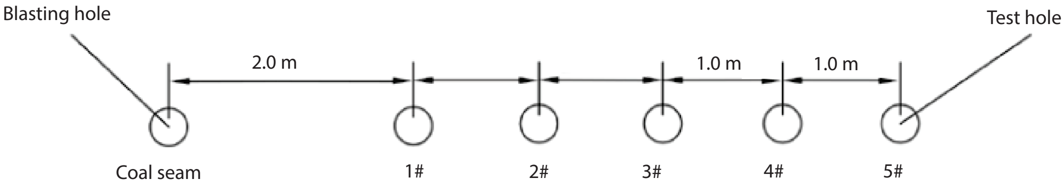

Figure 6. The lay-out of test borehole by loose blasting

After drilling, the gas concentration of the borehole is continuously observed. Considering the measurement error of new borehole caused by the grounding stress and the construction disturbance, the loose blasting test for each borehole is carried out when the gas emission from the borehole is relatively stable, and the gas concentration of the borehole is tracked before and after drilling. The test period is 275 day. It can be seen from fig. 7 that after blasting, the gas concentration of hole ($1^{\#}$) and hole ($2^{\#}$) increases obviously, the hole ($1^{\#}$) increases from 12.9-24.8%, and the hole ($2^{\#}$) from 9.5-23.5%. The average growth is 119.5%. At the same time, since the distance between the hole ($1^{\#}$) and hole ($2^{\#}$) is 0.5 m, the increase reaction time of the gas concentration is delayed, which can be seen from the hole ($3^{\#}$).

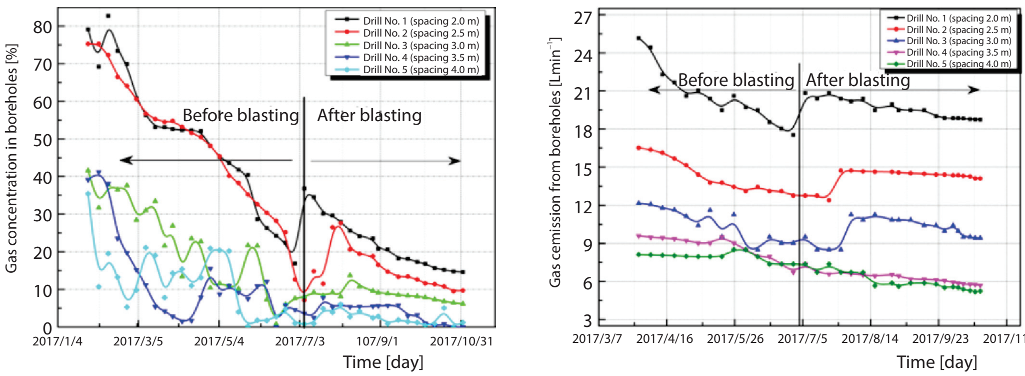

Figure 7. Variation curve of gas volume fraction and emission; (a) gas volume fraction, (b) gas quantity

The gas concentration of the hole ($2^{\#}$) can gain increase due to the blasting, while the gas concentration of hole ($3^{\#}$) increases slightly because of the 4.0 m distance between the hole ($3^{\#}$) and the blasting hole. The gas concentration of hole ($3^{\#}$) increases from 4.7-8.9%, which shows the hole ($3^{\#}$) is also affected by the blasting shock wave. The gas concentration of the hole ($4^{\#}$) and hole ($5^{\#}$) does not fluctuate, while the gas concentrations of the holes are continuously attenuated. During the subsequent continuous observation, there is still no abnormal gas emission. Therefore, it can be judged that it is not affected by the blasting. The same change law of gas emission amount and its concentration in the borehole can also be found. Before and after blasting, the change of gas emission is obvious. With the increase of the distance from the blasting hole, the gas emission amount of hole ($1^{\#}$) and hole ($2^{\#}$) increases significantly, however, hole ($3^{\#}$) has a small increase. The lag effect is also showing up among them. From the field test, the effective influence range of the blasting can be regard as between 3.0 m and 3.5 m.

Conclusion

In this work, the influence range of deep-hole loose blasting was simulating. The results show that the effective influence range of loose blasting reaches between 3.5 m and 4.0 m, which is verified by field test. Base on the simulation and on-site tracking test with the time of near 275 day, the *stress relief and flow enhancement effect* is obvious under the effect of loose blasting measures. The lag effect of gas migration is revealed during blasting.

Acknowledgment

This work was supported by the National Key Research and Development Program of China (2018YFC0808100), the National Science Foundation of China (51604269), Post-doctoral Science Foundation funded project of China (2017M621877), Chinese academy of engineering advisory research project of China (2017-ZD-003), Hebei State Key Laboratory of Mine Disaster Prevention (KJZH2017K11) and Open Research Fund of State Key Laboratory of Geomechanics and Geotechnical Engineering (Z015008).

Nomenclature

f_i – volume force, [Nm^{-3}]
Q_p – sink source term, [$kgm^{-3}s^{-1}$]
S – displacement, [m]
v – Poisson's ratio, [–]

Greek symbols

σ_{ij} – stress tensor, [MPa]
σ_H – volume stress, [Nm^{-2}]

References

[1] Zhou, F. B., *et al.,* Recent Developments in Coal Mine Methane Extraction and Utilization in China: A Review, *Journal of Natural Gas Science and Engineering, 31* (2016), Apr., pp. 437-458
[2] Xia, T. Q., *et al.,* A Fully Coupled Coal Deformation and Compositional Flow Model for the Control of the Pre-Mining Coal Seam Gas Extraction, *International Journal of Rock Mechanics and Mining Sciences, 72* (2014), Dec., pp. 138-148
[3] Ma, G. W., *et al.,* Numerical Simulation of Blasting-Induced Rock Fractures, *International Journal of Rock Mechanics and Mining Sciences*, *45* (2007), 6, pp. 966-975
[4] Yang, X. J.*,* A New Integral Transform Operator for Solving the Heat-Diffusion Problem, *Applied Mathematics Letters, 64* (2017), Feb., pp. 193-197
[5] Yang, X. J.*, et al.,* A New Numerical Technique for Local Fractional Diffusion Equation in Fractal Heat Transfer, *Journal of Non-Linear Science and Applications, 9* (2016), 10, pp. 5621-5628
[6] Drzewiecki, J., *et al.,* Dynamic Events in Roof Strata-Occurrence and Prevention, *Coal Science and Technology Magazine*, *1* (2008), 1, pp. 55-57
[7] Lekontsev, Y. M., *et al.,*Directional Hydraulic Fracturing in Difficult Caving Roof Control and Coal Degassing, *Journal of Mining Science, 50* (2015), 5, pp. 914-917
[8] Konicek, P., *et al.,* Long-Hole Destress Blasting for Rock burst Control during Deep Underground Coal Mining, *International Journal of Rock Mechanics and Mining Sciences*, *61* (2013), 5, pp. 141-153
[9] Sawmliana, C., *et al.,* A New Blastability Index for Hard Roof Management in Blasting Gallery Method, *Geo-Technical and Geological Engineering*, *30* (2012), 6, pp. 1357-1367
[10] Song, J., *et al.,* Micromechanical Modelling of the Dynamic Fracture Process during Rock Blasting, *International Journal of Rock Mechanics and Mining Sciences & Geo-Mechanics Abstracts*, *33* (1996), 3, pp. 387-394

[11] Zuo, J. P., *et al.,* A Study of Fractal Deep-Hole Blasting and Its Induced Stress Behavior of Hard Roof Strata in Bayangaole Coal Mine, China, *Advances in Civil Engineering*, *2019* (2019), ID 9504101
[12] He, F. L., *et al.,* Study on Depressurizing Control of the Surrounding Rock of a Roadway along Gob Area in Sub-Level Caving Mining, *Journal of China Coal Society*, *25* (2000), 6, pp. 589-592
[13] Li, H., *et al.,* Experimental Analysis of Rock Mass Rupture Range by Mine Production Blasting, *Blasting*, *33* (2016), 2, pp. 45-48
[14] Sun, K. M., *et al.,* Numerical Simulation on Crack Propagation Law of Pre-Splitting Explosion in Lowly Permeable Coal Seam, *Blasting*, *31* (2014), 1, pp. 32-37
[15] Furlong J. R, *et al.,* Modelling the Dynamic Load/Unload Behavior of Ceramics under Impact Loading RDA-TR-0030-0001, R and D Associates, Arlington, VA., USA, 1990

Paper submitted: June 7, 2018
Paper revised: September 12, 2018
Paper accepted: March 10, 2019